Available online at www.sciencedirect.com
ScienceDirect
Journal of Solid State Chemistry 179 (2006) 3024–3032
JOURNAL OF SOLID STATE CHEMISTRY
www.elsevier.com/locate/jssc

Crystal structure of $Mg_{0.65}Sc_{0.35}D_x$ deuterides studied by X-ray and neutron powder diffraction

M. Latroche[a,*], P. Kalisvaart[b], P.H.L. Notten[b,c]

[a]*Laboratoire de Chimie Métallurgique des Terres Rares—UPR209—CNRS, 2-8 rue Henri Dunant 94320 Thiais, Cedex, France*
[b]*Eindhoven University of Technology, 5600 MB Eindhoven, The Netherlands*
[c]*Philips Research Laboratories, 5656 AE Eindhoven, The Netherlands*

Received 21 March 2006; received in revised form 23 May 2006; accepted 28 May 2006
Available online 3 June 2006

Abstract

The structural properties of the $Mg_{0.65}Sc_{0.35}D_x$ deuterides have been investigated by X-ray and neutron powder diffraction at different deuterium content ($0 \leqslant x \leqslant 2.2$ D/f.u.). The metallic phase adopts a pseudo-CsCl structure (*Pm*-3*m* space group (SG); $a = 3.5921(2)$ Å) that transforms upon hydrogenation into a face centered cubic (FCC) phase involving an elongation of the *c*-axis, a shrinkage of the *a*-axis and a re-ordering of the metallic atoms. The fully hydrided compound (2.2 D/f.u.) adopts a cubic structure (*Fm*-3*m* SG; $a = 4.8087(7)$ Å) and deuterium is located in fully occupied tetrahedral sites and partially filled (24%) octahedral sites. Upon desorption, a two-phase domain appears with coexistence of a hydrogen-rich (1.55 D/f.u.) and a hydrogen-poor (0.85 D/f.u.) phase (*Fm*-3*m* SG; $a = 4.7598(3)$ and $4.6936(3)$ Å, respectively). All deuterium atoms are located in the tetrahedral sites with different occupancy factors: 77% for the H-rich phase and 43% for the H-poor phase. The appearance of a plateau in the pressure–composition-isotherm curve measured at 573 K confirms this two-phase behavior. The structural properties of the $Mg_{0.65}Sc_{0.35}D_x$ system are discussed and compared with other body centered cubic (BCC) alloys adopting the same structure.

Keywords: Intermetallics; Hydrogen storage materials; Gas–solid reaction; Crystal structure; Neutron diffraction

1. Introduction

The application of $LaNi_5$-type hydrogen storage materials in rechargeable Nickel Metal-Hydride batteries has become a great commercial success in the last decades. Almost half of the small rechargeable battery market is currently devoted to this battery system, while the potentials in hybrid electrical vehicles are even greater. In addition, efficient hydride-forming materials are crucial for storage applications in Fuel Cells.

A new class of materials composed of much lighter constituents and thus revealing a much higher hydrogen storage capacity per weight than the conventional $LaNi_5$ materials has recently been discovered and investigated at the Philips Research Laboratories [1–4]. It has been found that a specific fluorite type of Mg-based compounds can store up to five times (close to 6 wt%!) the amount of hydrogen compared to that of the conventional $LaNi_5$, making these new materials very attractive for extremely high-capacity energy storage devices.

MgSc alloys with compositions ranging from 50 to 100 at% Mg were studied electrochemically [1] and it was found that the favorable discharge kinetics were retained up to 80 at% Mg. The improvement of the (de)hydriding kinetics compared to pure Mg was thought to be due to the fact that the hydrided form of the material assumed the fluorite-type structure of pure ScH_2 instead of the rutile structure of MgH_2. The fluorite structure was confirmed for a composition of $Mg_{65}Sc_{35}$ and also for $Mg_{75}Sc_{25}$ by ex situ X-ray diffraction (XRD) [5].

Because Sc is very expensive, attempts to find cheaper substitutes were also undertaken. Both Ti and V form dihydrides with the same fluorite structure as ScH_2 and therefore were likely candidates. A study on Mg–Ti and Mg–V thin films, showed a similar improvement of the

*Corresponding author. Fax: +33 1 49 78 12 03.
E-mail address: michel.latroche@iscsa.cnrs.fr (M. Latroche).

0022-4596/$ - see front matter © 2006 Elsevier Inc. All rights reserved.
doi:10.1016/j.jssc.2006.05.032

discharge kinetics compared to pure MgH_2 for compositions $Mg_{80}Ti_{20}$ and $Mg_{80}V_{20}$ [2]. A more elaborate study on the Mg–Ti system revealed that the composition dependence of the discharge capacity was quite similar to MgSc, also showing a maximum around 80 at% Mg. [6] Therefore, the crystal structure of the resulting hydride does indeed seem to play a crucial role in determining the (de)hydrogenation kinetics of the material.

In this paper, the first step was to study by neutron diffraction (ND) the Mg–Sc sublattice in order to precisely determine the position and occupancy factors of the Mg and Sc atoms. In a second step, ND has been performed to locate deuterium (hydrogen) atomic positions in the fully hydrided $Mg_{0.65}Sc_{0.35}$ compound. Finally, electrochemical [1,5] and gas-phase measurements provide evidence for the existence of a two-phase region during dehydriding the alloy. This phase transformation is assumed to be fluorite-to-sphalerite, but from XRD analysis, this transition is only visible from the appearance of two face centered cubic (FCC) structures with different lattice constants [5]. From ND analysis, the D/H atom positions can be determined and the nature of the phase transition will be confirmed. Accordingly, four samples have been measured by ND at different deuterium concentrations. To investigate the materials' behavior upon desorption, a hydrided material was heated in a thermogravimetric analyzer until all reversible hydrogen had been released. The crystal structures of the resulting material were analyzed by X-ray diffraction and its behavior compared to that of other well-known hydride-forming materials. Normally, the MgSc material is doped with a few at% of Pd to ensure good (electrochemical) discharge kinetics, even at room temperature [1]. However, Pd will form a number of ternary compounds with Mg and Sc [5], which may interfere with the structure determination of the main phase. Therefore, the investigation on the unhydrided material was conducted on a Pd-free sample, while the partial desorption study was carried out on a Pd-containing sample, enabling the use of a more moderate desorption temperature.

2. Experimental methods

2.1. Sample preparation and characterization

The $Mg_{0.65}Sc_{0.35}$ samples were prepared by weighing the constituent elements in a molybdenum crucible, which was then sealed in an arc furnace under a high-purity Argon atmosphere to withstand the high vapor pressure of Mg. The sample was then annealed at 1150 °C for 18 h. The alloy was subsequently quenched and annealed at 450 °C for 4 days. This procedure was used to prepare both alloys with and without Pd. About 2.4 at% of Pd was added to enhance the hydrogen sorption kinetics, for both gas phase and electrochemical hydrogenation/deuteration.

Composition and homogeneity of the samples have been controlled by XRD on a Bruker AXS D8 $\theta-\theta$ diffractometer (CuK_α, Bragg–Brentano geometry, 2θ range 20–120°, step size 0.02°, backscattered rear graphite monochromator), electron probe microanalysis (EPMA Camebax SX100) and transmission electron microscopy coupled with energy dispersive X-ray analysis have been performed (EDX-TEM). The microscope is a JEOL 2000FX, 200 kV equipped with STEM and an EDX detector Si(Li) ISIS 200 from Oxford Instruments. Measurements have been obtained using Cliff–Lorimer quantification with absorption correction (thickness 100 nm).

Deuteration of the $Mg_{0.65}Sc_{0.35}Pd_{0.02}$ alloy has been performed at the Philips Research Laboratories in Eindhoven by exposing the powder to deuterium gas under the following conditions ($T = 300$ °C, $P = 13$ MPa) to ensure complete deuteration of the sample. The unhydrided material has very good air stability, both as metal lumps and in powder (~40 μm diameter) form. As for all alkali-metal alloys, contact with relatively acidic (pH < 12) media should be avoided for both the metal and the hydrided material. For this latter one, contact with water vapor should also be avoided as much as possible, but the stability in dry air, even when fully charged, is quite good. No significant changes in the material occur in up to several months of room-temperature storage, so the material can safely be assumed to be unaltered over the experimental timescale.

Thermogravimetric analysis (TGA) has been performed with a Mettler Toledo SDTA 851^e Thermogravimetric Analyser. A sample of about 50 mg was heated in a 70 μL alumina cup at a rate of 5 °C/min under flowing Argon at 25 mL/min. First a measured weight-vs.-T curve of an empty cup was determined under the same conditions and eventually subtracted from the measurement done on the sample to filter out any artifacts caused by changes in the density of the surrounding atmosphere.

ND measurements were carried out at the Laboratoire Léon Brillouin in Saclay. The diffraction patterns were recorded on the 3T2 instrument in the range $6° < 2\theta < 120°$ by step of 0.05° ($\lambda = 1.225$ Å). All patterns were refined with the Rietveld method using FULLPROF program [7]. Between each ND measurements, the sample was heated to 300 °C and desorbed step by step using the Sievert's method.

3. Results

3.1. Pd-free sample

Chemical analysis has been carried out by EPMA and shows a homogeneous sample with an average composition $Mg_{0.651(3)}Sc_{0.349(3)}$ in good agreement with the expected one ($Mg_{0.65}Sc_{0.35}$). The XRD experiments show that the pattern can be indexed in the cubic space group $Pm\text{-}3m$ with a cell parameter of 3.5940(6) Å. Some small lines indexed in the P mode are not compatible with the I mode and this confirms that the structure cannot be considered as purely body centered cubic (BCC), since in a pure BCC

Table 1
Crystallographic structure for the Pd-free sample $Mg_{0.65}Sc_{0.35}$ obtained from powder neutron diffraction analysis (Space group *Pm*-3*m*). Occupancy factors for sites 1*a* and 1*b* were constraints to $\delta N^{Sc}_{1a} = -\delta N^{Mg}_{1a} = -\delta N^{Sc}_{1b} = \delta N^{Mg}_{1b}$

Atom	Wyckoff position	(*x*,*y*,*z*)	*B* (Å^2) (*σ*(*B*))	*N* (*σ*(*N*))
Mg	1*a*	(0,0,0,)	1.72 (5)	0.384 (6)
Sc				0.616 (6)
Mg	1*b*	($\frac{1}{2}$, $\frac{1}{2}$, $\frac{1}{2}$)	1.29 (6)	0.916 (6)
Sc				0.084 (6)
$a = 3.5921(2)$ Å, $V = 46.350(4)$Å^3				
	$R_p = 4.4\%$	$R_{wp} = 6.3\%$	$R_{Bragg} = 6.7\%$	$\chi^2 = 9.6$

structure, reflections for which the sum of the indices is odd are not present. From the ND measurement performed at room temperature, the distribution between the two different sites available for Mg and Sc in the structure has been refined. The total amount of Sc and Mg atoms was fixed to the nominal composition with $N^{Sc}_{1a} + N^{Sc}_{1b} = 0.70$ and $N^{Mg}_{1a} + N^{Mg}_{1b} = 1.30$ where $N_i{}^M$ stands for the occupancy factor for metal *M* sitting on site *i*. Occupancy factors for both Mg and Sc atoms and both sites 1*a* and 1*b* were constraints ($\delta NSc_{1a} = -\delta N^{Mg}_{1a} = -\delta N^{Sc}_{1b} = \delta N^{Mg}_{1b}$ where $\delta N^M{}_i$ stands for the shift of the parameters $N^M{}_i$) so that only one parameter was used to refine the atomic repartition within the two sites. Scandium is almost exclusively located on site 1*a* (0,0,0) whereas Mg is distributed over the two sites 1*a* and 1*b* ($\frac{1}{2}$, $\frac{1}{2}$, $\frac{1}{2}$). Results of the refinement are given in Table 1 and the refined diffraction pattern is shown in Fig. 1.

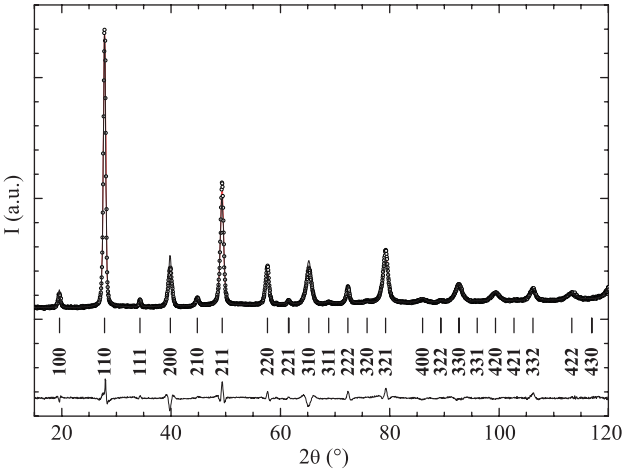

Fig. 1. Refined diffraction pattern of the Pd-free sample $Mg_{0.65}Sc_{0.35}$ obtained from powder neutron diffraction analysis (measured (dots), calculated (solid line) and difference curves (below); Vertical bars correspond to diffraction line positions of the $Mg_{0.65}Sc_{0.35}$ phase).

3.2. Pd-containing sample

For this sample, a small amount (2.4 at%) of palladium has been added in order to enhance the kinetics of the deuteration process. Before starting the NPD experiments, the metallic sample has been studied by EPMA for a better understanding of the element distribution. From X-ray imaging of the sample surface, it is observed that Sc is evenly distributed throughout the sample; Pd is located mainly in the grain boundaries whereas Mg is seen only in the main phase (Fig. 2). Some deuterated grains of the $Mg_{65}Sc_{35}Pd_{2.4}D_{2.2}$ sample have been also studied by EDX-TEM in order to check the composition. The quantitative analysis confirms the presence of the three elements Mg, Sc and Pd. The mean values are: Mg 67.54 ± 1.80 at%; Sc 32.18 ± 1.73 at%; Pd 0.28 ± 0.22 at% leading to the composition $Mg_{0.675}Sc_{0.322}Pd_{0.003}$. It is worthwhile to note that the magnesium-to-scandium ratio is in good agreement with the nominal ratio. However, palladium is observed in very low quantities, about eight times less than expected from the nominal composition.

3.3. Pd-containing deuterated sample (2.2 D/f.u)

The deuterated sample has been studied, using combined X-ray and ND analysis. The diffraction patterns show the presence of a main cubic phase that can be indexed in the space group *Fm*-3*m* with a cell parameter of 4.8087(7) Å. Such transformation into a CaF_2-type structure is commonly observed in dihydrides of BCC metals such as V and Nb and for Ti, V solid solutions upon hydrogenation [8,9]. The partial Mg/Sc ordering seen in the non-deuterated phase is no longer observed here and both atoms are randomly substituted on site 4*a*. Two different sites are available for hydrogen in the structure: one tetrahedron in position 8*c* and one octahedron in position 4*b* (Fig. 3). The tetrahedral sites are found almost fully occupied by deuterium with an occupation factor of 97.7% leading to 1.954 ± 0.031 D per metal in this position. The second octahedral site is only partly filled by deuterium with 0.243 ± 0.008 D per metal. The overall composition is estimated to be $Mg_{0.65}Sc_{0.35}D_{2.2(4)}$. In addition, diffraction patterns show a broad line around 36° that can be attributed to a cubic secondary phase $ScPd3D_x$ with a cell parameter of 4.092(4) Å. The relative amount for this phase cannot be accurately estimated due to its small quantity and its poor crystallinity. Results of the joint refinement are given in Table 2 and refined diffraction patterns are shown in Fig. 4.

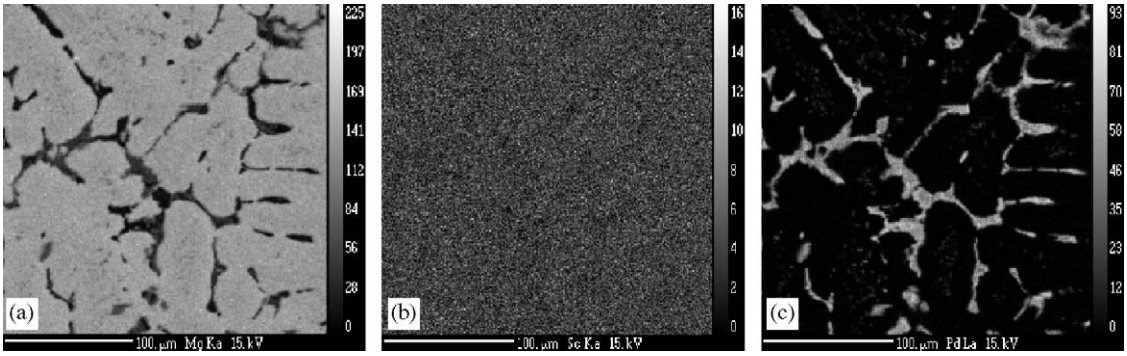

Fig. 2. X-ray imaging of (a) MgK^{α} (b) ScK^{α} (c) PdL^{α}, at the surface of the sample $Mg_{65}Sc_{35}Pd_{2.4}$. The brighter zones correspond to the area where the element is present.

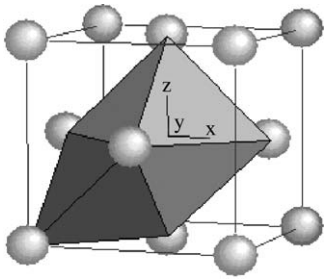

Fig. 3. 3D view of the crystal structure of the deuterated sample showing the two different sites available for hydrogen within the cell: tetrahedral site 8*c* ($\frac{1}{4}$, $\frac{1}{4}$, $\frac{1}{4}$) is shown in black, octahedral site 4*b* ($\frac{1}{2}$, $\frac{1}{2}$, $\frac{1}{2}$) in grey and (Mg,Sc) atoms 4*a* (0,0,0) as white spheres (*Fm*-3*m* space group).

3.4. Pd-containing deuterated sample (1.69 D/f.u)

Starting from the fully charged deuteride (2.2 D/f.u.), the sample has been desorbed by the Sievert's method at 300 °C to a composition close to 1.69 D/f.u. under a pressure of 0.064 MPa and has then been cooled down to room temperature. From combined X-ray and ND analysis, it appears that the cubic phase is preserved but with a smaller cell parameter of 4.7583(3) Å. Only the tetrahedral sites are partially occupied with 1.55 ± 0.02 deuterium per metal whereas the octahedral sites are nearly empty. If one assumes that the accuracy of the solid–gas measurements is about 5–6% (1.69 ± 0.10 D/f.u.), a reasonable agreement is obtained with the value obtained form neutron refinement. Results of the joint refinement are given in Table 3.

3.5. Pd-containing deuterated sample (1.2 D/f.u)

The sample was additionally desorbed at 300 °C to the composition 1.2 D/f.u. under a final pressure of 0.005 MPa and cooled down to room temperature. Analyses of the diffraction patterns show the presence of two cubic phases with two different cell parameters, $a = 4.6936(3)$ and 4.7598(5) Å, respectively. Such an observation can be attributed to the coexistence of two deuterated phases in equilibrium. Accordingly, the patterns were refined assuming two deuterides. Results of the refinement (Table 4) give a deuterium-poor (0.85 D/f.u.) and a deuterium-rich phase (1.55 D/f.u.) with all deuterium atoms located in the tetrahedral sites. From the relative amount of each phase (42 and 58 wt%, respectively), the average concentration is estimated around 1.25 D/f.u., in good agreement with the 1.2 D/f.u. obtained from the gas phase measurements. The refined ND pattern is shown in Fig. 5.

3.6. Thermal desorption of a Pd-free hydrogenated sample

Finally, a thermal desorption analysis of a Pd-free hydrogenated sample was performed between room temperature and 520 °C (Fig. 6) starting from the composition $Mg_{0.65}Sc_{0.35}H_{2.25}$. The TGA curve shows that hydrogen is mainly released between 300 and 450 °C. Above this temperature, no mass loss is observed and the sample cannot be further desorbed. According to the measured sample weight change, the composition obtained above 450 °C is equal to $Mg_{0.65}Sc_{0.35}H_{0.75}$.

The X-ray diffraction pattern of the sample after desorption is shown in Fig. 7. Analysis of the pattern shows the presence of two main phases: a ScH_2 hydrided phase (*Fm*-3*m* space group, Sc in 4*a*, H in 8*c*, $a = 4.7796(1)$ Å, $R_B = 5.5\%$) and a Mg phase ($P6_3/mmc$ space group, Mg in 2*c*, $a = 3.2228(1)$ Å, $c = 5.2191(2)$ Å, $R_B = 7.9\%$).

Beside these two main phases, small peaks attributed to various oxides or hydroxides are observed (MgO, ScO, Sc_2O_3 and ScOOH mainly) and are attributed to some oxygen contamination during the heat treatment at elevated temperature. From the refinement of the X-ray data, the relative amount of the ScH_2 and Mg phases is estimated at 48.8(2) and 51.1(3) wt%, respectively. It is worth to note that the decomposition reaction $Mg_{0.65}Sc_{0.35}H_{0.7} \rightarrow 0.35\ ScH_2 + 0.65$ Mg should lead to a weight ratio of 51 and 49 wt%, respectively in good agreement with the present data.

4. Discussion

The first point about the metallic sample concerns the position and occupancy factors of the Mg and Sc atoms.

Table 2
Crystallographic structure of deuterated $Mg_{0.65}Sc_{0.35}Pd_{0.02}$ obtained from joint refinement of neutron and X-ray diffraction patterns for the sample containing 2.2 D/f.u. (Space group *Fm*-3*m*)

Atom	Wyckoff position	(*x*,*y*,*z*)	*B* (Å^2) ($\sigma(B)$)	*N* ($\sigma(N)$)
$Mg_{0.65}Sc_{0.35}D_x$	*Fm*-3*m*			
Mg	4*a*	(0,0,0)	0.81 (3)	0.65 (fixed)
Sc				0.35 (fixed)
D (O)	4*b*	($\frac{1}{2}$, $\frac{1}{2}$, $\frac{1}{2}$)	5.20 (8)	0.243 (8)
D (T)	8*c*	($\frac{1}{4}$, $\frac{1}{4}$, $\frac{1}{4}$)		0.977 (15)
		$a = 4.8087$ (7) Å	$V = 111.19$ (3)Å^3	
		ND_$R_{Bragg} = 6.6\%$		
		X-ray_$R_{Bragg} = 2.0\%$		
$ScPd_3D_y$	*Pm*-3*m*			
Sc	1*a*	(0,0,0)	0.81 (3)	1.0 (fixed)
Pd	3*c*	(0, $\frac{1}{2}$, $\frac{1}{2}$)		1.0 (fixed)
D	1*b*	($\frac{1}{2}$, $\frac{1}{2}$, $\frac{1}{2}$)	5.20 (8)	1.0 (fixed)
D	3*d*	($\frac{1}{2}$, 0 0)		1.0 (fixed)
		$a = 4.092(4)$ Å	V = 68.5(1)Å^3	
		ND_$R_{Bragg} = 9.1\%$		
		X-ray_$R_{Bragg} = 9.6\%$		
		ND_$R_p = 3.3\%$	26 refined	
		$R_{wp} = 4.4\%$	parameters	
		X-ray_$R_p = 7.6\%$	22 + 51(ND) +	
		$R_{wp} = 9.8\%$	12 + 30 (X-ray) reflections	
		$\chi^2 = 2.6$		

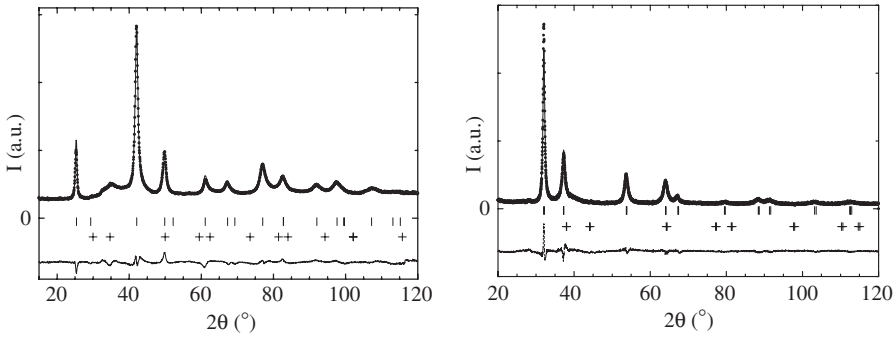

Fig. 4. Refined neutron (left) and X-ray (right) diffraction patterns observed for the Pd-containing deuterated sample containing 2.2 D/f.u (measured (dots), calculated (solid line) and difference curves (below)). Markers correspond to diffraction line positions of each phase: (|) $Mg_{0.65}Sc_{0.35}D_{2.2}$; (+) $ScPd_3D_x$.

According to our refinement, the structure can be described as a pseudo-CsCl one with a pseudo-($Sc_{0.62}Mg_{0.38}$) atom on 1*a* and pure Mg on 1*b* (see Table 1). It is already known that the compound MgSc adopts a pure CsCl-type structure with Sc atoms located on the 1*a* site and Mg on 1*b* site [10]. When increasing the amount of Mg, the magnesium atoms progressively substitute the scandium ones. When the total amount of Mg reaches 65 at%, the structure is no longer stable [11] and a two-phase equilibrium with the hexagonal hP2 magnesium solid solution appears.

Strikingly, the Mg/Sc ordering is no longer observed in the hydride phases. Two effects are observed upon hydrogenation. Firstly, the transformation into the CaF_2-type structure of the metal sublattice occurs. When going from CsCl-type to FCC-type structure, the following changes of parameters are expected: $a' = a + b$; $c' = c$. Starting from the metallic phase cubic parameter ($a = 3.592$ Å) and after loading 2.2 D/f.u, a cubic cell parameter with $a' = 4.809$ Å is obtained so the *c*-axis expands from 3.592 to 4.809 Å (+33.9%) whereas the *a*-axis shrinks from 5.079 Å (3.592. $\sqrt{2}$) to 4.809 Å (−5.3%). The overall volume expansion is equal to 19.9%. Elongation along the *c*-axis leading to the FCC structure has already been reported for BCC metals and solid solutions upon hydrogenation [8,9]. However, for some systems like (Ti,V,Mn), a pseudo-cubic intermediate phase corresponding to a small tetragonal distortion ($c/a = 0.91$) is reported for the first mono-hydride but that is not observed in the present study. In addition, a re-ordering of the atomic

Table 3
Crystallographic structure of deuterated $Mg_{0.65}Sc_{0.35}Pd_{0.02}$ obtained from joint refinement of neutron and X-ray diffraction patterns for the sample containing 1.69 D/f.u. (Space group *Fm*-3*m*)

Atom	Wyckoff position	*(x,y,z)*	*B* (Å^2) (*σ*(*B*))	*N* (*σ*(*N*))
$Mg_{0.65}Sc_{0.35}D_x$	*Fm*-3*m*			
Mg	4*a*	(0,0,0)	1.16 (3)	0.65 (fixed)
Sc				0.35 (fixed)
D (T)	8*c*	$(\frac{1}{4},\frac{1}{4},\frac{1}{4})$	1.78 (5)	0.772 (12)
D (O)	4*b*	$(\frac{1}{2},\frac{1}{2},\frac{1}{2})$		−0.016 (7)
		$a = 4.7583$ (3) Å	$V = 107.74$ (1)Å^3	
		ND_$R_{Bragg} = 2.9\%$		
		X-ray_$R_{Bragg} = 2.5\%$		
$ScPd_3D_y$	*P m*-3*m*			
Sc	1*a*	(0,0,0)	0.81 (3)	1.0 (fixed)
Pd	3*c*	$(0,\frac{1}{2},\frac{1}{2})$		1.0 (fixed)
D	3*d*	$(\frac{1}{2},0,0)$	5.20 (8)	0.66 (fixed)
		$a = 4.1858(71)$ Å	$V = 73.3(2)$Å^3	
		ND_$R_{Bragg} = 5.8\%$		
		X-ray_$R_{Bragg} = 4.3\%$		
		ND_$R_p = 3.1\%$	25 refined	
		$R_{wp} = 3.8\%$	parameters	
		X-ray_$R_p = 8.4\%$	23 + 54(ND) +	
		$R_{wp} = 10.6\%$	12 + 32(X-ray)	
		$\chi^2 = 5.0$	reflections	

Table 4
Crystallographic structure of deuterated $Mg_{0.65}Sc_{0.35}Pd_{0.02}$ obtained from joint refinement of neutron and X-ray diffraction patterns for the sample containing 1.2 D/f.u. (Space group *Fm*-3 *m*)

Atom	Wyckoff position	*(x,y,z)*	*B* (Å^2) (*σ*(*B*))	*N* (*σ*(*N*))
$Mg_{0.65}Sc_{0.35}D_x$	*Fm*-3*m*			
Mg	4*a*	(0,0,0)	1.13 (2)	0.65 (fixed)
Sc				0.35 (fixed)
D (T)	8*c*	$(\frac{1}{4},\frac{1}{4},\frac{1}{4})$	1.26 (3)	0.426 (7)
D (O)	4*b*	$(\frac{1}{2},\frac{1}{2},\frac{1}{2})$		0.006 (5)
		$a = 4.6936$ (3) Å	V = 103.40 (1)Å^3	
		ND_$R_{Bragg} = 2.9\%$	42 (1) wt%	
		X-ray $R_{Bragg} = 4.2\%$		
$Mg_{0.65}Sc_{0.35}D_{x'}$	*F m*-3*m*			
Mg	4*a*	(0,0,0)	1.13 (2)	0.65 (fixed)
Sc				0.35 (fixed)
D (T)	8*c*	$(\frac{1}{4},\frac{1}{4},\frac{1}{4})$	1.26 (3)	0.777 (12)
D (O)	4*b*	$(\frac{1}{2},\frac{1}{2},\frac{1}{2})$		−0.066 (7)
		$a = 4.7598$ (5) Å	$V = 107.84$ (2)Å^3	
		ND_$R_{Bragg} = 2.8\%$	58 (1) wt%	
		X-ray_$R_{Bragg} = 4.5\%$		
$ScPd_3D_y$	*Pm*-3*m*			
Sc	1*a*	(0,0,0)	1.13 (2)	1.0 (fixed)
Pd	3*c*	$(0,\frac{1}{2},\frac{1}{2})$		1.0 (fixed)
D	3*d*	$(\frac{1}{2},0,0)$	1.26 (3)	0.5 (fixed)
		$a = 4.227(5)$ Å	$V = 75.53(14)$Å^3	—
		ND_$R_{Bragg} = 4.2\%$	wt% not refined	
		X-ray_$R_{Bragg} = 3.0\%$		
		ND_$R_p = 2.5\%$	32 refined parameters	
		$R_{wp} = 3.0\%$		
		X-ray_$R_p = 7.1\%$	22 + 23 + 54(ND) + 1	
		$R_{wp} = 9.0\%$	2 + 15 + 32(X-ray)	
		$\chi^2 = 1.9$	reflections	

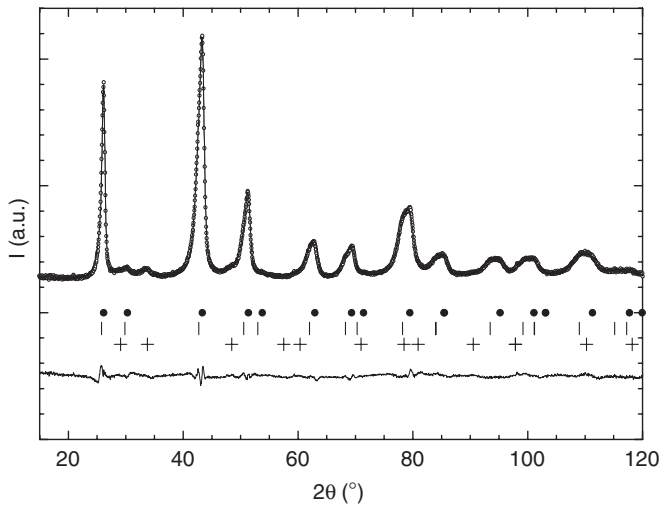

Fig. 5. Refined neutron diffraction pattern observed for the Pd-containing deuterated sample, containing 1.2 D/f.u (measured (dots), calculated (solid line) and difference curves (below)). Markers correspond to diffraction line positions of each phase: (●) $Mg_{0.65}Sc_{0.35}D_{0.85}$; (|) $Mg_{0.65}Sc_{0.35}D_{1.55}$; (+) $ScPd_3D_x$.

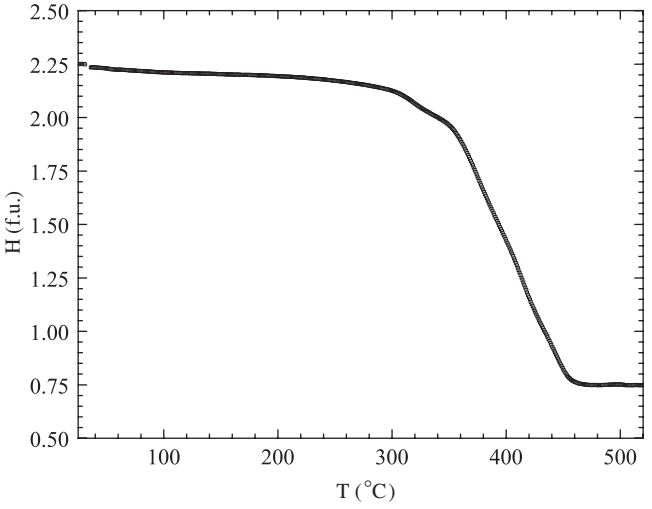

Fig. 6. TGA curve of the Pd-free hydrogenated sample $Mg_{0.65}Sc_{0.35}H_{2.25}$, measured between room temperature and 520 °C. The composition above 450 °C is equal to $Mg_{0.65}Sc_{0.35}H_{0.75}$.

distribution is observed. Indeed, the body-centered atom located on the 1*b* site made of pure Mg in the metallic phase becomes a face-centered atom in the CaF_2-type structure but with a random distribution of Mg vs. Sc which implies strong rearrangements of the metallic atoms. Such hydrogen-induced atomic rearrangements have already been observed in other systems like $MgPd_3$ [12], for which the transformation from Zr_3Al-type α-$MgPd_3$ into $AuCu_3$-type β-$MgPd_3$ is reported after hydrogenation at moderate pressure and heating up to 750 K. Such process can apparently also take place in the present $Mg_{0.65}Sc_{0.35}$ compound. However, the TGA experiments have shown that part of the capacity is irreversible and that thermal desorption of the sample does not allow to decrease the

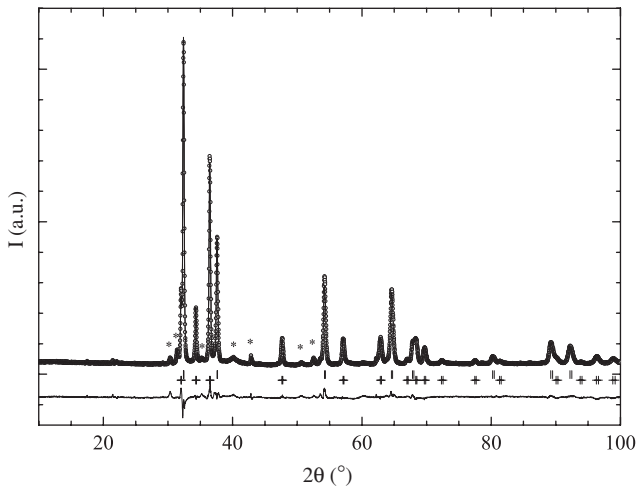

Fig. 7. X-ray diffraction pattern for a Pd-free hydrogenated sample after thermal desorption at 500 °C showing measured (dots), calculated (solid line) and difference curves (below). Vertical bars correspond to diffraction lines of the ScH_2 phase (*Fm*-3*m* space group) and crosses to that of the Mg phase ($P6_3/mmc$ space group). Stars indicate small amounts of oxides or hydroxides (MgO, ScO, Sc_2O_3 and ScOOH) included in the refinement.

capacity below 0.7 H/M without decomposing the material into ScH_2 and metallic Mg.

To perform hydrogenation of the sample with good kinetics, a little amount (2.4 wt%) of palladium was added to the main phase. From our analysis, it is clear that Pd does not enter into the structure of the $Mg_{0.65}Sc_{0.35}$ compound but remains at the grain boundaries as clearly observed in Fig. 2. However, possible formation of a metallic phase with scandium cannot be excluded from this analysis. Indeed, a bump is observed around 36°(2θ) in the ND pattern of the Pd-containing deuterated sample (2.2 D/f.u) though the existence of such a secondary phase is not so obvious when looking to the X-ray diffraction pattern. This is probably due to the additional scattering contribution to ND coming from deuterium and scandium that have scattering length much larger than that of palladium (6.67 and 12.29 fm, respectively, vs. 5.91 fm for Pd). It means that this secondary phase contains both palladium and scandium and should absorb hydrogen since the intensity of the bump varies with the total deuterium amount. Among the possible Pd–Sc phases, we have chosen to attribute this bump to the cubic phase $ScPd_3D_x$ though it is difficult to fully conclude on that matter due to the very large broadening of the diffraction peaks and to the relatively small amount for this secondary phase.

Concerning the main phase, deuterium was found to fully occupy the 8*c* tetrahedral (T) site and partially the 4*b* octahedral (O) one leading to an overall D content of 2.2 D/f.u (see Table 2). As this compound stands in the solid solution domain of the beta branch, larger capacity can be expected by raising the pressure in order to increase the occupation factor of the O site. However, it is important to note that fast H diffusion in such compounds can be achieved only for partially occupied hydrogen sites

in order to allow 'hopping' of hydrogen atoms between two neighboring sites. As the T site is fully occupied, fast motion of D atoms can occur only through the O site. Such mobility of the deuterons in the octahedral position may explain the high value of the displacement parameter B (5.20 Å^2) observed for the D sites. However, further studies using quasi-elastic neutron scattering, for example, are necessary to finally conclude on that matter.

When decreasing the D content by solid/gas desorption, it is observed that the octahedral site is no longer occupied and the occupancy factor of the tetrahedral site decreases down to 77% (Table 3). At this stage, further desorption leads to a two-phase domain with two hydrides in equilibrium containing 0.85 and 1.55 D/f.u. and corresponding to 43% and 77% of occupancy factor for the tetrahedral site, respectively (see Table 4). Such existence of a plateau is also confirmed by the partial PCT curve measured upon desorption on the sample at 300 °C (573 K) that exhibits a plateau-like behavior between 1.2 and 1.69 and an increasing β branch above (Fig. 8), in accordance with electrochemical measurements carried out at RT [1,5]. It is worthwhile to note that the equilibrium pressure at 573 K is close to 0.06 MPa on the plateau.

Upon deuteration, a volume expansion is observed as a function of deuterium content. As the FCC cell contains twice the number of metallic atoms of the pseudo-CsCl cell, it is more convenient for comparison to look at the cell volume per metal. This evolution is shown in Fig. 9. For low D content, a volume increase of 11.5% is obtained in the range 0–0.85 D/f.u. On the plateau, the discrete volume expansion (i.e. the volume difference between the two deuterated phases in equilibrium on the plateau) is limited to +4.8% followed by an additional +3.6% in the β solid solution branch. It is worth to note that the volume expansion is less important in the range 0.85–2.2 D/f.u. (+8.4%) despite a large capacity variation (+1.35 D/f.u.). As the reversible part of the system is expected to take

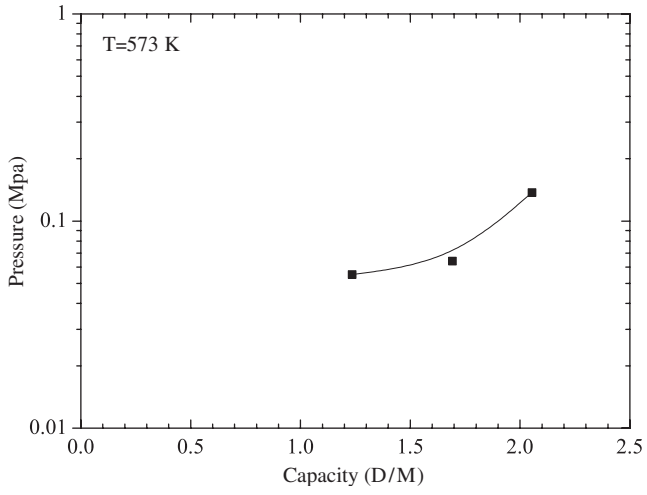

Fig. 8. Partial pressure–composition–temperature (PCT) curve measured upon desorption for the Pd-containing $Mg_{0.65}Sc_{0.35}$ deuterated sample at 573 K.

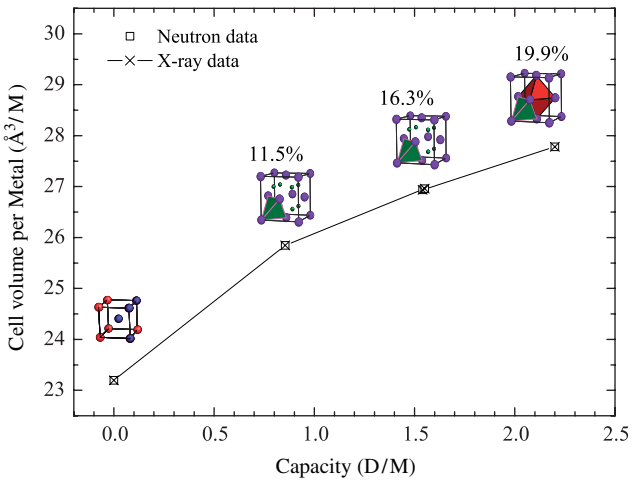

Fig. 9. Evolution of the cell volume per metal as a function of the deuterium content for the Pd-containing $Mg_{0.65}Sc_{0.35}$ deuterated sample. The volume expansions $\Delta V/V$ are given in % in the figure together with the schematic crystal structures.

place at the higher H/D contents [1–4], such low volume expansion should generate very few strains in the compounds and could lead to enhanced cycle life [13].

5. Conclusions

The crystal structure of a Pd-containing $Mg_{65}Sc_{35}$ compound has been studied upon hydrogenation. The metallic phase adopts a pseudo-CsCl-type structure. When hydrogenated, the structure changes from pseudo-CsCl to FCC involving an elongation along the c-axis, shrinkage along the a-axis and a re-ordering of the metallic atoms. A two-phase domain is subsequently observed between 0.85 and 1.55 D/f.u. with two hydrides in equilibrium, corresponding to 43% and 77% of the occupancy factor for the tetrahedral sites, respectively. Above this value, a β branch appears, leading to a fully occupied tetrahedral site and a partially filled octahedral site, allowing fast diffusion of H atoms. The hydrogenation reaction is fully reversible in the range 0.85 and 2.25 H/f.u. but thermal desorption of the sample below 0.7 H/f.u. leads to decomposition into ScH_2 and Mg.

Acknowledgments

This research was performed as part of the Sustainable Hydrogen Programme of Advanced Chemical Technologies for Sustainability (ACTS). The authors wish to thank Mrs. F. Briaucourt for technical assistance, Mr. E. Leroy for EPMA and TEM analysis and Mrs. Bourée-Vigneron for the neutron diffraction measurements.

References

[1] P.H.L. Notten, M. Ouwerkerk, H. van Hal, D. Beelen, W. Keur, J. Zhou, H. Feil, J. Power Sour. 129 (2004) 45.

[2] R.A.H. Niessen, P.H.L. Notten, Electrochem. Solid-State Lett. 8 (10) (2005) A534.
[3] R.A.H. Niessen, P.H.L. Notten, J. Alloys Compounds 404–406 (2005) 457.
[4] R.A.H. Niessen, P. Vermeulen, P.H.L. Notten, Electrochim. Acta 51 (12) (2006) 2427.
[5] W.P. Kalisvaart, R.A.H. Niessen, P.H.L. Notten, J. Alloys Compounds 417 (2006) 280.
[6] P. Vermeulen, R.A.H. Niessen, P.H.L. Notten, Electrochem. Commun. 8 (1) (2005) 27.
[7] J. Rodríguez-Carvajal, Physica B 192 (1993) 55.
[8] Y. Nakamura, E. Akiba, J. Alloys Compounds 311 (2000) 317–321.
[9] Y. Nakamura, K.I. Oikawa, T. Kamiyama, E. Akiba, J. Alloys Compounds 316 (2001) 284–289.
[10] O. Schob, E. Parthé, Acta Cryst 19 (1965) 214.
[11] A. A. Nayeb Hashemi, J. B. Clark, In: T. B. Massalski (Ed.), Binary Alloy Phase Diagrams,vol. 3, second ed., ASM International, Materials Park, OH, 1990, p. 2545.
[12] H. Kohlmann, G. Renaudin, K. Yvon, C. Wannek, B. Harbrecht, J. Solid State Chem. 178 (4) (2005) 1292.
[13] P.H.L. Notten, J.L.C. Daams, R.E.F. Einerhand, J. Alloys Compounds 210 (1994) 233–241.